Fluoroolefins as Peptide Mimetics. 2. A Computational Study of the Conformational Ramifications of Peptide Bond Replacement

Brian E. McKinney and Joseph J. Urban*

Chemistry Department, United States Naval Academy, 572 Holloway Road, Annapolis, Maryland 21402

Received: October 1, 2009; Revised Manuscript Received: November 17, 2009

The design of peptide mimetic compounds is greatly facilitated by the identification of functionalities that can act as peptide replacements. The fluoroalkene moiety has recently been employed for that purpose. The purpose of this work is to examine the conformational ramifications of replacing peptide bonds with fluoroalkene moieties, thus generating peptidomimetics. The alanine dipeptide analogue (ADA) was chosen as a model compound. Three peptidomimetic systems were investigated including one generated by replacement of both peptide bonds of ADA, designated as DFA, and those generated by the single replacement of the C-terminal peptide bond and N-terminal peptide bond, designated as CFA and NFA, respectively. Conformations for all three systems were generated by exhaustive Monte Carlo searching. Relative conformational energies were calculated at the MP2/aug-cc-pVTZ/MP2/aug-cc-pVDZ (for DFA), MP2/-aug-cc-pVTZ//MP2/6-311+G(d,p), B3LYP/6-31+G(d)//B3LYP/6-31+G(d), and MMFF levels of theory. Aqueous phase conformational preferences were determined through calculations making use of continuum hydration models. The results indicate that replacement of both peptide bonds of ADA generates a peptidomimetic with conformational preferences where extended conformations are favored and the conformational profile is relatively insensitive to the nature of the surrounding medium. This is in contrast to ADA where the conformational preferences depend highly on the surrounding medium and where folded conformations with intramolecular hydrogen bonds are important in the absence of an interacting solvent. CFA and NFA are found to exhibit conformational preferences that do in some ways more closely resemble those of the alanine dipeptide analogue. This is particularly true in the case of NFA where interactions between the NH and CF groups are reminiscent of the intramolecular hydrogen bonding possible in ADA.

Introduction

The use of compounds that mimic peptides is widespread in pure and applied research of biochemical systems. Peptidomimetics have great utility in fields ranging from medicinal chemistry to nanomaterials. For example, while peptides are attractive agents for probing the structure and function of a drug receptor, they have very limited potential as pharmaceutical agents themselves. They have a tendency to exhibit poor bioavailability and short physiological lifetimes. The problem lies in the fact that peptidic compounds are readily destroyed by hydrolytic enzymes such as peptidases.[1] Thus, a common strategy is to exploit the structural diversity offered by peptides to discover lead compounds and then create nonpeptidic versions that mimic the peptide's structure and function. Representative examples of fluorolefin-based pepditomimetics that have been employed as enzyme inhibitors are shown below (Figure 1). Beyond drug discovery efforts, biomimetic strategies have also been applied in areas as diverse as the development of biologically inspired nanoscale devices,[2] conformationally rigid peptide analogues designed to promote β turns,[3] and model compounds for the study of cell membrane activity.[4]

The design of an effective peptide mimetic hinges on finding a suitable replacement for the peptide bond. One strategy that has been adopted is to simply replace the peptide bond with an alkene bond.[7,8] This is a logical approach given that the peptide bond is considered to have significant partial double-bond character as evidenced by its shorter bond distance and higher barrier to rotation (as compared to a purely single C−N bond). Replacement of a peptide bond with an alkene should produce a compound that is of roughly similar size and shape as the original peptide (the term "peptide isostere" is often used to describe such compounds). But, the electrostatic potential (distribution of charge on the molecular surface) that the mimetic presents to the intended receptor may not be well represented by the nonpolar alkene. As a result, the use of fluoroolefins has been suggested because the electronegativity of the fluorine atom is expected to create an isostere that has a more accurate representation of the electrostatic potential of the original peptide (see Figure 2). For example, Bartlett has investigated the effectiveness of fluoroalkenes as inhibitors of thermolysin,[9] and Welch and co-workers employed fluoroolefin peptide mimetics

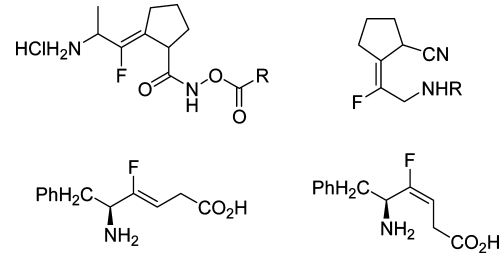

Figure 1. Examples of fluoroolefin peptide mimetics. The structure on the top left represents compounds previously studied by Welch[1] and co-workers, and the one on the top right has been investigated by Augustyns and co-workers.[5] The bottom structures have been investigated by Niida et al.[6]

* To whom correspondence should be addressed. E-mail: urban@usna.edu. Telephone: 410-293-6605. Fax: 410-293-2218.

10.1021/jp9094535
Published on Web 12/14/2009

Report Documentation Page

Form Approved
OMB No. 0704-0188

1. REPORT DATE	2. REPORT TYPE	3. DATES COVERED
17 NOV 2009		**00-00-2009 to 00-00-2009**

4. TITLE AND SUBTITLE	5a. CONTRACT NUMBER
Fluoroolefins as Peptide Mimetics. 2. A Computational Study of the Conformational Ramifications of Peptide Bond Replacement	5b. GRANT NUMBER
	5c. PROGRAM ELEMENT NUMBER
6. AUTHOR(S)	5d. PROJECT NUMBER
	5e. TASK NUMBER
	5f. WORK UNIT NUMBER
7. PERFORMING ORGANIZATION NAME(S) AND ADDRESS(ES) **United States Naval Academy,Chemistry Department,572 Holloway Road,Annapolis,MD,21402**	8. PERFORMING ORGANIZATION REPORT NUMBER
9. SPONSORING/MONITORING AGENCY NAME(S) AND ADDRESS(ES)	10. SPONSOR/MONITOR'S ACRONYM(S)
	11. SPONSOR/MONITOR'S REPORT NUMBER(S)

12. DISTRIBUTION/AVAILABILITY STATEMENT
Approved for public release; distribution unlimited

13. SUPPLEMENTARY NOTES

14. ABSTRACT

15. SUBJECT TERMS

16. SECURITY CLASSIFICATION OF:			17. LIMITATION OF ABSTRACT	18. NUMBER OF PAGES	19a. NAME OF RESPONSIBLE PERSON
a. REPORT **unclassified**	b. ABSTRACT **unclassified**	c. THIS PAGE **unclassified**	**Same as Report (SAR)**	**11**	

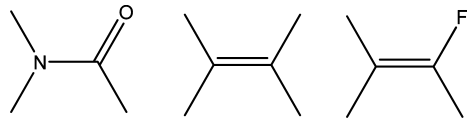

Figure 2. Peptide and olefin and fluoroolefin mimetics. Olefin and fluoroolefin peptide mimetics have been used in the study of several important biochemical and biological systems.

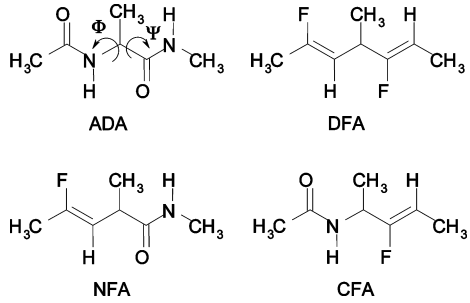

Figure 3. Systems under study in this work include the peptide mimics that result from the replacement of both peptide bonds of the alanine dipeptide analogue (ADA) with fluoroalkene moieties (DFA) as well as the mimics resulting from replacement of only the N-terminal peptide bond (NFA) and the C-terminal peptide bond (CFA). The backbone torsional angles Φ and Ψ are depicted for the ADA compound. The same terms, Φ and Ψ, are applied to the corresponding torsions in the other compounds.

in the inhibition of the dipeptidyl peptidase IV enzyme (DPP IV) and the cyclophilin enzyme.[10] Ceiplak and co-workers investigated the effectiveness of both olefins and fluoroolefins as inhibitors of the HIV-1 protease enzyme.[11] Miller and co-workers have employed olefin isosteres as mechanistic probes in the development of peptide-based enantioselective catalysts.[7] There has also been a great deal of work directed toward the synthesis[9,10,12−14] of biologically active fluoroalkenes which is further evidence of their potential as mechanistic probes and therapeutic agents.

In a previous work published in this journal,[15] we employed high-level computational methods to compare the structures, electrostatic potentials, and intermolecular hydrogen bonding abilities of simple amides representing models of peptides to their fluoroalkene counterparts serving as model compounds for peptidomimetics (*N*-methylacetamide compared to 2-fluoro-2-butene, for example). In the present work, we extend this study to an examination of the ramifications of peptide bond replacement, by fluoroalkene mimics, on the conformational preferences of model peptides. The system chosen to serve as the model compound is the well-studied alanine dipeptide analogue (ADA) shown in Figure 3. There have been numerous computational[16] and experimental[17,18] studies of the conformational distribution of ADA reported in the literature as this system has served as a prototype for the study of protein folding and in the development of computational methods designed to model proteins. The effect of solvent medium on the conformational distribution has also been investigated. The alanine dipeptide analogue possesses two peptide bonds flanking an alanine residue (capped with *N*-methyl and acetyl groups). We have investigated the conformational preferences of the peptidomimetic generated by replacement of both peptide bonds with fluoroalkenes (DFA) as well as the two generated by single replacement of the N-terminal (NFA) and C-terminal peptide bonds CFA (see Figure 3).

Computational Methods

Conformational searching was done using the Monte Carlo multiple minimum (MCMM)[19,20] routines of the Maestro(v. 6.5)/Macromodel-Batchmin(8.6)[21] suite of programs. The number of Monte Carlo steps for the searches was 500 000. Energy minimization was performed with the MMFF94s force field, which is the Macromodel implementation of the MMFF force field.[22−26] Parameters for the Monte Carlo (MC) search were generated using the automatic setup routine. This results in inclusion of all rotatable bonds in the search with peptide bonds limited to a trans configuration. Newly found structures are compared against previously found ones by rigid superposition with a maximum distance of 0.25 Å between heavy atoms allowed in order for the structures to be considered equal. The unique conformers that were obtained from the MC searches provided the input structures for optimizations with the quantum mechanical methods. MC searches were also run in the aqueous medium by use of the GB/SA[27] continuum hydration model as implemented in Macromodel. The quantum mechanical studies were conducted with the Gaussian03[28] suite of programs. Complete geometry optimizations were carried out for all systems with the 6-311+G(d,p) basis set at the MP2[29] level of theory and with the 6-31+G(d) basis set using the B3LYP[30,31] hybrid density functional. Single-point energies at the MP2/aug-cc-pVDZ and MP2/aug-cc-pVTZ levels of theory were obtained for all minima resulting from the MP2/6-311+G(d,p) optimizations. For the DFA systems, optimizations at MP2/aug-pVDZ were also performed. To include the effect of solvent in the quantum mechanical calculations, the default IEF-PCM[32−35] aqueous continuum model of Gaussian03 was used. All minima were confirmed as such through vibrational frequency calculations.

In conducting these studies, every effort was made to be as exhaustive as possible in terms of the inclusion of input structures that could potentially lead to conformational minima. This was handled though the use of extensive Monte Carlo searching to provide initial geometries for optimization with quantum mechanical methods with Gaussian03 as outlined above. But, it was also emphasized in the manner in which the Gaussian03 calculations were approached. For example, all of the output structures from the MC studies served as input structures for optimizations with MP2/6-311+G(d,p) and B3LYP/6-31+G(d). However, if a structure was obtained at B3LYP that was not among the set of those obtained with MP2, it would also be explicitly subjected to optimization at the MP2 level. This includes the aqueous phase versus the gas phase calculations as well. For example, if the set of minima obtained from aqueous phase (GB/SA) Monte Carlo searches included structures that were not among the set obtained from the gas phase searches (where no solvent model was used), these new structures would be subjected to both gas and aqueous phase Gaussian03 optimizations. Thus, whenever a method (gas phase, aqueous phase, MMFF, B3LYP, MP2) generated a novel structure, that structure was subjected to optimization with all methods.

Results

Alanine Dipeptide Analogue: Double Peptide Bond Replacement (DFA). Figure 4 shows the conformations that were identified as minima in the gas phase for the double replacement compound DFA. Table 1 shows the Φ, Ψ dihedral angles from the MP2/6-311+G(d,p) and MP2/aug-cc-pVDZ optimized geometries, the dipole moments, and the relative conformational energies at a variety of levels of theory. The following designations are used to denote the levels of theory that have been investigated: MP2-I = MP2/6-311+G(d,p)//MP2/6-311+G(d,p), MP2-II = MP2/aug-cc-pVDZ //MP2/6-311+G(d,p), MP2-III = MP2/aug-cc-pVTZ//MP2/6-311+G(d,p), MP2-IV =

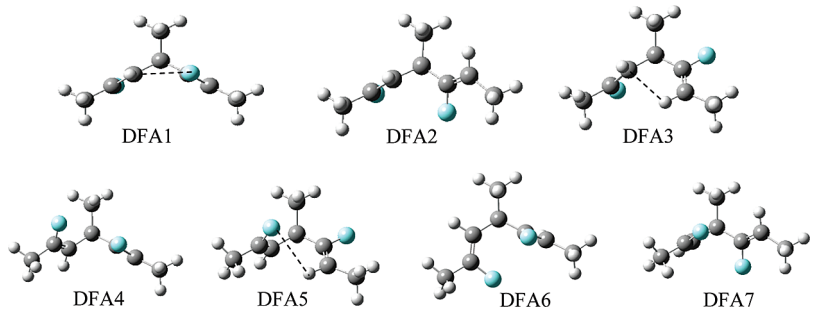

Figure 4. MP2/6-311+G(d,p) geometries for the energy minima that were found for DFA in the gas phase. Nearly identical results (not shown) were found with MP2/aug-cc-pVDZ.

TABLE 1: Relative Energies (Δ*E*, in kcal/mol) and Torsion Angles for Gas Phase Conformations of DFA

				Δ*E*						
	Φ[a]	Ψ[a]	μ[b]	MP2-I[c]	MP2-II[d]	MP2-III[e]	MP2-IV[f]	MP2-V[g]	B3LYP[h]	MMFF[i]
DFA1	−118.9[j]	118.3[j]	0.706[j]	0.00	0.00	0.00	0.00	0.00	0.00	0.00
	−122.1[k]	*118.7*[k]	*0.643*[k]							
DFA2	−114.4	−114.3	2.74	0.74	0.48	0.35	0.46	0.35	0.89	2.01
	−117.6	*−114.9*	*2.66*							
DFA3	−108.6	0.3	3.03	0.61	0.25	0.13	0.24	0.13	0.68	2.07
	−109.3	*1.0*	*3.12*							
DFA4	94.9	114.5	2.78	2.84	2.61	2.61	2.60	2.59	3.14	2.09
	98.6	*114.5*	*2.71*							
DFA5	78.4	−10.5	3.01	2.69	1.95	2.06	1.92	2.03		
	75.0	*−10.9*	*2.97*							
DFA5b	112.5	−19.5							3.19	
DFA5m	118.8	−59.6								2.51
DFA6	−24.0	123.9	2.40	3.04	2.67	2.69	2.66	2.68		3.91
	−27.7	*126.4*	*2.27*							
DFA7	65.9	−117.1	1.74	2.69	2.22	2.21	2.21	2.20	3.33	
	64.2	*−118.7*	*1.71*							

[a] Dihedral angle, in degrees. [b] Dipole moment, in debye. [c] MP2-I = MP2/6-311+G(d,p)//MP2/6-311+G(d,p). [d] MP2-II = MP2/aug-cc-pVDZ//MP2/6-311+G(d,p). [e] MP2-III = MP2/aug-cc-pVTZ//MP2/6-311+G(d,p). [f] MP2-IV = MP2/aug-cc-pVDZ//MP2/aug-cc-pVDZ. [g] MP2-IV = MP2/aug-cc-pVTZ//MP2/aug-cc-pVDZ. [h] B3LYP/6-31+G(d)//B3LYP/6-31+G(d). [i] As implemented in Maestro (v6.5)/Macromodel-Batchmin (v8.6). [j] MP2/6-311+G(d,p) geometries. [k] Italicized values are from MP2/aug-cc-pVDZ geometries.

MP2/aug-cc-pVDZ//MP2/aug-cc-pVDZ, and MP2-V = MP2/aug-cc-pVTZ//MP2/aug-cc-pVDZ. In order to assess the reliability of more computationally efficient methods, results were also obtained with the B3LYP/6-31+G(d) density functional method and the Merck molecular force field (MMFF)[22−26] as implemented in Maestro/Macromodel. Table 2 shows the thermochemical corrections.

In a comprehensive study of conformational preferences of peptide model compounds, Kaminsky and Jensen[36] endorsed the MP2/aug-cc-pVTZ level of theory as capable of highly accurate (∼1 kJ) conformational energies. In their study, MP2/aug-cc-pVDZ was employed for final refinement of geometries (following initial optimizations and characterization of minima via frequency calculations at the MP2/6-31G(d) level). We have employed geometry optimization (and characterization via frequency calculation) at both the MP2/6-311+G(d,p) and MP2/aug-cc-pVDZ levels of theory. For the DFA system, the results indicate a negligible difference between the geometries and subsequent single-point energies at higher levels of theory. The dihedral angles obtained with the two methods are within a few degrees of each other. Comparison of the MP2-II results to those of MP2-IV, and MP2-II to those of MP2-V, reveals agreement in conformational energies that are within hundredths of a kcal/mol. Because of the increased computational efficiency (especially in the frequency calculations), the MP2/6-311+G(d,p) level of theory was employed for geometries and frequencies in the subsequent systems under study in this work.

We are interested in determining if the conformational preferences of DFA reported above resemble those that have been previously reported for the alanine dipeptide analogue (ADA) or the standard backbone conformations found in proteins. Table 3 provides a summary of the very comprehensive computational study of the conformational preferences of the alanine dipeptide analogue in the gas phase and in aqueous (and ether) solutions reported by Wang and Duan.[16] Much of the results of that work are corroborated in the more recent work

TABLE 2: MP2/6-311+G(d,p) and MP2/aug-cc-pVDZ-Calculated Relative Energies and Thermochemical Corrections (in kcal/mol) for the Gas Phase Conformations of DFA

	Δ*E*	Δ(E+ZPE)	Δ*E*(298)	Δ*H*(298)	Δ*G*(298)
DFA1	0.00[a]	0.00	0.00	0.00	0.00
	0.00[b]	*0.00*	*0.00*	*0.00*	*0.00*
DFA2	0.74	0.81	0.75	0.75	0.97
	0.46	*0.58*	*0.50*	*0.50*	*0.75*
DFA3	0.61	0.59	0.56	0.56	0.77
	0.24	*0.27*	*0.22*	*0.22*	*0.43*
DFA4	2.84	2.97	2.93	2.93	3.02
	2.60	*2.80*	*2.73*	*2.72*	*2.89*
DFA5	2.69	2.76	2.71	2.71	3.04
	1.92	*2.07*	*1.99*	*1.99*	*2.56*
DFA6	3.04	2.95	2.93	2.93	3.05
	2.66	*2.61*	*2.59*	*2.59*	*2.46*
DFA7	2.69	2.77	2.71	2.71	3.16
	2.21	*2.36*	*2.25*	*2.25*	*2.82*

[a] Geometry optimization and frequency calculation at MP2/6-311+G(d,p). [b] Italicized values derived from geometry optimization and frequency calculations at MP2/aug-cc-pVDZ.

TABLE 3: Literature[a] MP2/cc-pVTZ//MP2/6-31G(d,p)-Calculated Φ, Ψ Values and Relative Energies in Isolation and in the Aqueous Phase for the Alanine Dipeptide Analogue

	gas phase				aqueous phase		
	Φ^b	Ψ^b	ΔE^c		Φ^b	Ψ^b	ΔE^c
$C7_{eq}$	−82.0	80.6	0.00	$C7_{eq}$	−86.3	90.1	0.92
C5 (β_L)[d]	−159.7	159.3	1.47	C5 (β_L)[d]	−156.4	143.8	0.00
α_R (α_L)[d]	−80.0	−20.0	3.27	α_R (α_L)[d]	−70.5	−32.1	0.08
α_L (α_D)[d]	63.2	35.4	4.52	β	−64.0	142.1	0.17
$C7_{ax}$	75.8	−62.8	2.50	α_L (α_D)[d]	59.4	41.1	1.27
β_2	−141.6	23.8	3.25	$C7_{ax}$	74.9	−54.3	2.69
α′ (δ_D)	−166.1	−36.7	6.07	β_2	−145.6	27.2	1.27
α_D (ϵ_D)	53.0	−133.4	4.75	α_D	55.6	−144.9	3.59
				α_D'	60.5	−170.9	4.08

[a] Results from the study of Wang and Duan.[16] [b] In degrees. [c] In kcal/mol. [d] The conformer names in parentheses are those used in the study of Kaminsky and Jensen.[36]

TABLE 4: Approximate Backbone Dihedral Angles for Common Protein Structural Motifs[a]

	Φ	Ψ
α_R helix (right-handed helix)	−57	−47
α_L helix (left-handed helix)	57	47
β sheet (parallel-chain pleated sheet)	−119	113
β_{anti} sheet (antiparallel-chain pleated sheet)	−139	135
collagen	−51	153
PII poly(L-proline) II	−78	149

[a] The standard dihedral angle values are taken from the IUPAC-IUB Commission on Biochemical Nomenclature[37] and also appear in standard texts.[38]

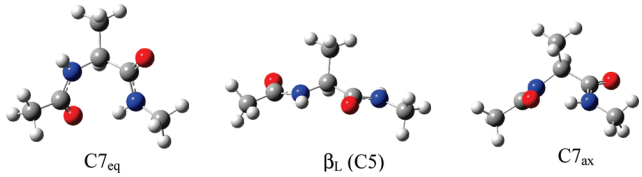

Figure 5. MP2/aug-cc-pVDZ geometries for the $C7_{eq}$, β_L (C5), and $C7_{ax}$ conformers from the study of Kaminsky and Jensen.[36]

of Kaminsky and Jensen.[36] We will refer to the results of these two studies throughout this work. In some instances, the same conformations are referred to by different names in these two studies as indicated in Table 3. Table 4 shows the standard Φ, Ψ angles associated with common structural motifs in proteins.

Overall, the gas phase conformational profile for the double-replacement peptidomimetc DFA does not closely resemble that which has been reported in the literature for the alanine dipeptide analogue (ADA). For example, the lowest-energy structure, DFA1, with its Φ, Ψ dihedral angle values of −118.9°, 118.3°, is rather extended. These values are close to the −119°, 113° values quoted for parallel β sheet structures (Table 4). For the alanine dipeptide analogue, the $C7_{eq}$ conformation (Figure 5) is found to be the lowest energy gas phase structure.[16,36] It has Φ,Ψ values of approximately −80°, 80° and is characterized by an intramolecular hydrogen bond between the N-terminal side carbonyl and the C-terminal side N−H resulting in a seven-membered ring. The C5 (β_L) conformer is the second-lowest energy structure. It is an extended conformer and possesses a favorable electrostatic arrangement of the N−H bond on the N-terminal side and the C═O bond on the C-terminal side (Table 1). When the peptide bond is replaced with a fluoroalkene, the hydrogen bond donor NH group is replaced by a CH moiety and the carbonyl acceptor is replaced by a C−F bond. On both the donor and acceptor counts, a significant reduction in hydrogen bonding ability is expected, and thus a perturbation of the conformational profile is expected. We have previously reported on the hydrogen bonding patterns of fluoroalkene peptidomimetics by examining their interactions with water molecules.[15] In fact, structures resembling hydrogen-bonded complexes were found with high-level ab initio calculations, but with significantly reduced binding energies compared to their peptide counterparts. Also, the geometries were quite different for the fluoroalkene−water complexes in that the C−F---H−O bond vectors were oriented in near orthogonal arrangements.

TABLE 5: Selected[a] Intramolecular Nonbonded Distances[b]

	gas	aqueous
DFA1: CH-F	2.709	2.758
DFA3: CH-C	2.534	2.552
DFA5: CH-F	2.895	2.859

[a] Distances are indicated with a dashed line in Figure 4. [b] In angstroms. MP2/6-311+G(d,p)-optimized geometries.

Thus, the absence of an intramolecular hydrogen bond results in an extended global minimum in the gas phase for DFA in contrast to ADA for which a folded structure with an intramolecular hydrogen bond is the global minimum in the absence of a solvent medium. Comparison of the remaining conformations of DFA (Table 1) and ADA (Table 3) reveals further differences. For example, the second-highest energy DFA conformer, DFA2, has Φ, Ψ values of −114.4°, −114.3°. This bears no resemblance to any of the ADA gas phase conformers in Table 3. It bears no great resemblance to any of the standard backbone conformations cited in Table 4 either. The closest agreement is to the right-handed α helix, but there is still a significant deviation from those Φ, Ψ values of −57°, −47°. DFA3 and DFA4 occupy regions of Φ,Ψ space that are unlike any populated by ADA. The closest standard conformation from Table 4 to DFA4 (94.9°, 114.5°) is the left-handed α helix at 57°, 47°. DFA5, at 78.4°, −10.5°, most closely resembles the $C7_{ax}$ conformation of ADA which is reported to be 2.3 kcal/mol above the ground state with Φ, Ψ values of 74°, −54° by Kaminsky,[36] with similar results reported by Wang and Duan.[16] DFA5b and DFA5m are variants that are only found with B3LYP/6-31+G(d) and MMFF, respectively. DFA6 is near the region between the $C7_{eq}$ and β regions with Φ, Ψ values of −24.0°, 123.9°. DFA7 at 65.9°, −117.1° is nearest the $C7_{ax}$ conformation.

While intramolecular hydrogen bonding is a determining factor in the case of ADA in the gas phase, analogous interactions do not appear to play a major role in the DFA system. Figure 4 shows a dashed line between atoms that are potentially engaged in an attractive interaction. These appear in conformations DFA1, DFA3, and DFA5, and the gas phase and aqueous phase values for the corresponding interatomic distances are recorded in Table 5. The conformational energies in Tables 1 and 2 reveal that, in the gas phase, there are three low-energy conformations that are nearly isoenergetic. At the highest levels of theory, DFA1, DFA2, and DFA3 are all within 0.5 kcal/mol of the global minimum, in terms of ΔE, zero-point energy corrected ΔE, and ΔE and ΔH at 298 K. The next lowest energy conformation is significantly higher in energy. DFA5 is 1.92 kcal/mol above the ground state at the MP2/aug-cc-pVDZ level and 2.03 at the MP2/aug-cc-pVTZ level for the MP2/aug-cc-pVDZ geometry with very similar results obtained using the MP2/6-311+G(d,p) optimized geometry. It is interesting to note that for those structures where there is close contact between C−H---F−C groups, the geometries are different than those of the cyclic hydrogen-bonded ADA $C7_{ax}$ and $C7_{eq}$ structures. For

TABLE 6: Relative Energies (ΔE, in kcal/mol) and Torsion Angles for Aqueous Phase Conformations of DFA

			ΔE						
	Φ[a]	Ψ[a]	MP2-I[b]	MP2-II[c]	MP2-III[d]	MP2-IV[e]	MP2-V[f]	B3LYP[g]	MMFF[h]
DFA1	−113.9[i]	118.7[i]	0.00	0.00	0.00	0.00	0.00	0.00	0.00
	−118.4[j]	*118.8*[j]							
DFA2	−113.6	−113.2	0.39	0.13	0.03	0.12	0.05	0.43	
	−114.9	*−114.4*							
DFA3	−108.0	−3.2	0.55	0.20	0.10	0.21	0.12	0.55	1.78
	−111.5	*−1.7*							
DFA4	89.2	114.2	2.32	2.05	2.12	2.09	2.10	2.57	1.06
	92.5	*114.6*							
DFA5	75.5	−7.8	2.78	2.00	1.89	2.00	2.10		
	73.9	*−9.1*							
DFA5b	112.5	−19.5						3.29	
DFA5m	116.1	−19.2						2.40	
DFA6	−19.7	123.0	2.38	1.99	2.05	2.01	2.06	2.75	2.02
	−20.9	*124.4*							
DFA7	62.7	−120.2	2.51	2.00	1.99	1.99	1.99	3.02	
	60.6	*−121.6*							

[a] Dihedral angle, in degrees. [b] MP2-I = MP2/6-311+G(d,p)//MP2/6-311+G(d,p). [c] MP2-II = MP2/aug-cc-pVDZ//MP2/6-311+G(d,p). [d] MP2-III = MP2/aug-cc-pVTZ//MP2/6-311+G(d,p). [e] MP2-IV = MP2/aug-cc-pVDZ//MP2/aug-cc-pVDZ. [f] MP2-V = MP2/aug-cc-pVTZ//MP2/aug-cc-pVDZ. [g] B3LYP/6-31+G(d)//B3LYP/6-31+G(d). [h] As implemented in Maestro (v6.5)/Macromodel-Batchmin (v8.6). [i] MP2/6-311+G(d,p) geometries. [j] Italicized values are from MP2/aug-cc-pVDZ geometries.

the fluorinated peptide mimics, the C−H and F−C bond vectors are skewed rather than arranged in a traditional hydrogen bond donor−acceptor arrangement as seen in the ADA case. This is reminiscent of the geometrical differences that are observed between water complexes of amides and fluoroalkenes that we reported previously.[15]

Inspection of the Table 1 data further indicates that there is reasonable agreement between the B3LYP/6-31+G(d) results and those obtained at the MP2 level with the aug-cc-pVDZ and aug-cc-VTZ basis sets. B3LYP/6-31+G(d) also predicts three low-energy conformations and three higher-energy conformations, although the spread among them is somewhat greater than that observed in the MP2 results. With B3LYP, the three low-energy conformations span a range of 0.89 kcal/mol, and the highest energy conformation is 3.33 kcal/mol above the ground state. But, the overall depiction of the conformational preferences of DFA in the gas phase is reasonably well reproduced with B3LYP/6-31+G(d). This is somewhat surprising as the poor performance of B3LYP and other density functional approaches with respect to dispersive interactions, which certainly play a role in determining conformational energies, has been noted in the literature.[39−41] The reasonably good agreement that is seen here may be attributable to the relatively small size of the systems under study and the very low polarizability of fluorine. The MMFF force field also predicts DFA1 to be the global minimum but also predicts all other structures to be more than 2 kcal/mol above the ground state. Thus, it misses the fact that DFA2 and DFA3 are also very low energy structures.

In the absence of specific interactions akin to hydrogen bonding, one might expect the relative energies of the DFA conformations in the gas phase to be highly correlated with dipole moment with structures possessing a favorable cancellation of bond dipoles, and thus a low dipole moment, to predominate in the gas phase. DFA1 is the lowest energy structure with all computational methods and also has the lowest dipole moment (calculated at MP2/aug-cc-pVDZ). But, DFA2 and DFA3 have significant dipole moments and are found, at least by the quantum mechanical methods, to be nearly as stable as DFA1 in the gas phase. The MMFF results do mirror the trend in dipole moment in that the least polar structure, DFA1, is found to be the minimum and all of the other structures, with significantly higher dipole moments, are found to be significantly higher in energy.

TABLE 7: MP2/6-311+G(d,p)//MP2/6-311+G(d,p)-Calculated Relative Energies and Thermochemical Corrections (in kcal/mol) for the Aqueous Phase Conformations of DFA

	ΔE	Δ(E+ZPE)	ΔE(298)	ΔH(298)	ΔG(298)
DFA1	0.00	0.00	0.00	0.00	0.00
DFA2	0.39	0.49	0.45	0.45	0.54
DFA3	0.55	0.54	0.54	0.54	0.32
DFA4	2.32	2.46	2.40	2.40	2.74
DFA5	2.78	2.92	2.86	2.86	3.23
DFA6	2.38	2.34	2.30	2.30	2.56
DFA7	2.51	2.64	2.56	2.56	2.97

We have also conducted calculations with the PCM[32−35] continuum aqueous solvation model (Tables 6 and 7). One would certainly not expect compounds such as DFA to be water-soluble. However, our motivation is simply to see how sensitive the conformational preferences of the fluoroalkene moiety are to dielectric effect of the surrounding medium. The PCM continuum model provides a convenient way to alter the medium, and the gas phase and aqueous phase simply provide benchmarks that span a wide range of possible environments. This is relevant to the fundamental question addressed in this work in terms of the conformational ramifications of peptide bond replacement in that one could imagine a larger oligopeptide, or even an engineered protein, that contains selected peptide bond replacements among a large array of native peptide bonds. In that scenario, the fluoroalkene might find itself in a variety of local environments, and thus the desire to examine the response in conformational preferences upon the variation of surrounding environment exists.

The native alanine dipeptide analogue exhibits a dependency on the surrounding environment with respect to its conformational preferences.[16,18,36,42−45] For example, the recent (2009) study of Lee et al. has proposed that ADA has an extended structure resembling a β strand or C5 in the solid state, a more cyclic structure with intramolecular hydrogen bonding such as $C7_{eq}$ or α_L in a nonpolar solvent (THF), and the polyproline II structure (P_{II}) in an aqueous environment.[43] Earlier works have

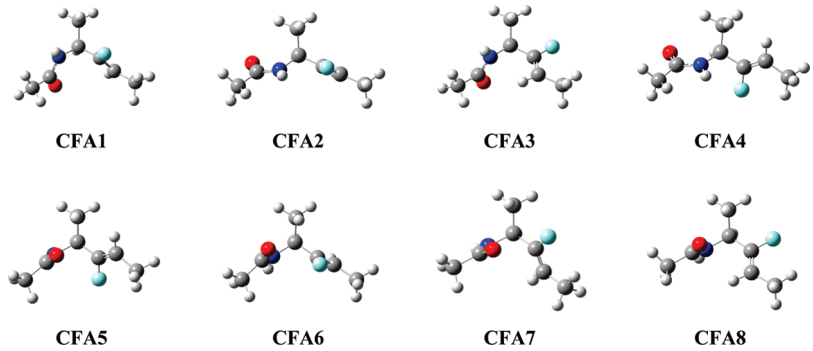

Figure 6. MP2/6-311+G(d,p) geometries for the energy minima that were found for CFA in the gas phase.

TABLE 8: Relative Energies (ΔE, in kcal/mol) and Torsion Angles for Gas Phase Conformations of CFA

				ΔE				
	Φ^a	Ψ^a	μ^b	MP2-I[c]	MP2-II[d]	MP2-III[e]	B3LYP[f]	MMFF[g]
CFA1	−80.9	113.1	2.30	0.00	0.00	0.00	0.00	
CFA2	−148.9	123.0	2.48	0.44	0.00	0.20		0.00
CFA3	−90.5	−5.26	4.83	1.38	0.84	1.16	1.36	
CFA4	−144.7	−115.0	4.34	1.50	0.77	0.93	1.21	2.11
CFA5	60.3	−120.4	2.48	2.70	2.42	2.28	3.50	4.44
CFA6	81.8	115.8	5.03	5.27	5.01	5.04	5.59	6.58
CFA7	52.3	66.5	5.34	5.90	5.48	5.54		7.33
CFA8	75.6	−7.12	4.32	4.00	3.38	3.43	4.61	7.84
CFA4m[h]	−157.0	−161.6						2.83

[a] Dihedral angle, in degrees. [b] Dipole moment, in debeye. [c] MP2-I = MP2/6-311+G(d,p)//MP2/6-311+G(d,p). [d] MP2-II = MP2/aug-cc-pVDZ//MP2/6-311+G(d,p). [e] MP2-III = MP2/aug-cc-pVTZ//MP2/6-311+G(d,p). [f] B3LYP/6-31+G(d)//B3LYP/6-31+G(d). [g] As implemented in Maestro (v6.5)/Macromodel-Batchmin (v8.6). [h] Found as a minimum only in MMFF optimizations. Torsion angles from the MMFF structure.

also noted a difference in the conformation between the aqueous phase, where the P_{II} structure is proposed to be important,[44] and environments lacking a highly interacting solvent (Ar matrix, nonpolar solvents) where $C7_{eq}$ and C5 are found to be important.[45] In the 2004 Duan and Wang study, the P_{II} structure was also identified as being important in aqueous solution especially when explicit waters were employed in the calculations which resulted in an increase in the importance of β (which resembles P_{II}) and a decreased importance of C5.[16]

DFA, on the other hand, is predicted to display very little variability in its conformational equilibrium with respect to the surrounding environment. In the aqueous phase, conformations DFA1, DFA2, and DFA3 are found to be essentially isoenergetic at the global minimum (Table 6), just as they are in the gas phase (Table 1). They are calculated to span a range of only 0.10 kcal/mol at the MP2/aug-cc-pVTZ//MP2/6-311+G(d,p) level with nearly identical results obtained at MP2/aug-cc-pVTZ//MP2/aug-cc-pVDZ. The remaining conformations are also very close in energy to each other and lie roughly 2 kcal/mol above the most favored conformer. Thus, the conformational profile of DFA in water is essentially identical to that in the gas phase. This situation is adequately captured by the B3LYP/6-31+G(d) calculations. However, as was seen in the gas phase, B3LYP predicts a slightly expanded range of energies with the low-lying conformations spanning a range of 0.55 kcal/mol and the highest-energy conformation located 3.29 kcal/mol above the ground state. MMFF with the GB/SA continuum solvent model does not reproduce the quantum mechanical results exactly. But, it does also predict the same conformer (DFA1) to be the global minimum in water as in the gas phase. However, a total of only five conformers are found in the aqueous phase with DFA4 1.06 kcal/mol above the ground state and the others 1.78−2.40 kcal/mol above the ground state.

Thus, the gas and aqueous phase conformational profiles of the doubly replaced peptide mimic DFA are predicted to be very similar to one another. The next important question to ask is whether the solvent-invariant conformational distribution of the mimic resembles the conformer distribution that the native alanine dipeptide exhibits in the gas phase, the aqueous phase, or neither. Clearly, DFA's conformational preferences are not very similar to the gas phase preferences of ADA because an intramolecular interaction analogous to the hydrogen bonding in $C7_{eq}$, which dominates the ADA conformational landscape in the gas phase and nonpolar solvents, is not observed for DFA. However, there are some similarites to the aqueous phase ADA conformer distribution in that the lowest energy conformations (DFA1 and DFA2) are rather extended.

Alanine Dipeptide Analogue: C-Terminal Peptide Bond Replacement (CFA). Figure 6 shows the conformations that were found to be minima in the gas phase for the peptide mimic where the C-terminal peptide bond has been replaced by a fluoroalkene moiety (CFA). Energetic information, for both the gas and aqueous phases, can be found in Tables 8 and 9 (with thermochemical corrections in the Supporting Information).

For CFA, four conformations are found to lie within just over 1 kcal/mol of the minimum (span a range of 1.16 kcal/mol with MP2-III). The lowest-energy structure, CFA1, exhibits Φ,Ψ values of −80.9° and 113.1°. It bears some resemblance to the $C7_{eq}$ conformation that was found as the gas phase global minimum for the alanine dipeptide analogue by Kaminsky and Jensen[36] and Wang and Duan.[16] The $C7_{eq}$ Φ,Ψ values in those studies were −82°, 76° and −82.0°, 80.6°, respectively. The next highest energy conformer, designated CFA2, is also somewhat similar to the second-highest ADA conformer, C5 (called β_L in the Kaminsky/Jensen study), with Φ,Ψ values of −80.9°, 113.1° compared to −161°, 157° in ADA.[36] However,

TABLE 9: Relative Energies (Δ*E*, in kcal/mol) and Torsion Angles for Aqueous Phase Conformations of CFA

			ΔE				
	Φ[a]	Ψ[a]	MP2-I[b]	MP2-II[c]	MP2-III[d]	B3LYP[e]	MMFF[f]
CFA1	−88.4	117.6	0.00	0.00	0.00	0.00	
CFA2							
CFA3	−93.2	−8.06	0.65	0.41	0.21	0.62	2.20
CFA4	−131.4	−114.3	0.96	0.49	0.43	0.45	1.33
CFA5	60.3	−130.5	2.64	2.13	2.28	3.31	3.51
CFA6	82.5	113.0	3.91	3.69	3.76	4.17	3.24
CFA7							4.41
CFA8	75.5	−0.22	3.60	3.02	3.10	4.28	5.20
CFA9m[g]	−153.6	117.5					0.00
CFA10m[g]	−144.7	21.1					2.06
CFA3m[g]	−115.6	0.60					2.25
CFA4m[g]	−152.5	−165.9					2.72
CFA11m[g]	−141.4	−27.9					2.74
CFA8m[g]	88.4	−47.6					5.63

[a] Dihedral angle, in degrees. [b] MP2-I = MP2/6-311+G(d,p)//MP2/6-311+G(d,p). [c] MP2-II = MP2/aug-cc-pVDZ//MP2/6-311+G(d,p). [d] MP2-III = MP2/aug-cc-pVTZ//MP2/6-311+G(d,p). [e] B3LYP/6-31+G(d)//B3LYP/6-31+G(d). [f] As implemented in Maestro (v6.5)/Macromodel-Batchmin (v8.6). [g] Found as a minimum only in MMFF optimizations. Angles reported in the table are MMFF values.

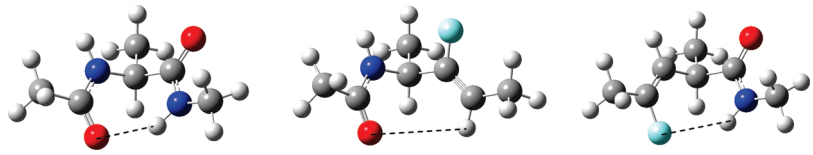

Figure 7. $C7_{eq}$ conformation of ADA (left) from the Kaminsky/Jensen study[36] at MP2/aug-cc-pVDZ compared to CFA2 (center) and NFA1 (right) from this work (MP2/6-311+G(d,p). The interatomic distances indicated by the dashed lines are 2.026 (left), 3.774 (center), and 2.407 (right) Å.

the β_L conformer was calculated to lie roughly 1.5 kcal/mol above the global minimum in the Kaminsk/Jensen and Wang/Duan studes, but CFA2 is seen here to be nearly isoenergetic with the ground state (0.44 and 0.20 kcal/mol above the ground state at the MP2-I and MP2-II levels, respectively). CFA2 was not found as a minimum with B3LYP, and it was the global minimum with MMFF.

DFA was not found to exhibit a $C7_{eq}$-like conformation. The ground state conformation for DFA is much more similar to the extended C5 (a.k.a β_L) ADA conformer. $C7_{eq}$ contains a close contact (2.026 Å) in the Kaminsky/Jensen[36] MP2/aug-cc-pVDZ structure) consistent with a C═O---H−N hydrogen bond. As described above, the calculations for DFA reveal that this type of interaction is not an important contributor to the DFA conformational landscape. It is interesting to note that in CFA, where the N-terminal side of the dipeptide analogue is peptidic and only the C-terminal side is fluoroolefinic, a conformation resembling the $C7_{eq}$ conformation is found to be the global minimum. Figure 7 shows a direct comparison of the $C7_{eq}$ conformation of ADA and the CFA1 conformation. The larger Ψ angle in CFA1 results in a much greater separation (3.274 Å) between the C═O and H−C moieties. One would certainly not expect the H−C of CFA to be as potent a hydrogen bond donor as the corresponding H−N of ADA. Also, the larger Ψ value orients the C−F bond more parallel to the opposing dipole of the C═O bond. But, clearly, there is a similarity between the two conformations. This is important because it suggests that a single fluoroalkene, incorporated into a longer polypeptide, might not perturb the conformational preferences of the system drastically. The fluoroalkene moiety provides the opportunity to examine a peptide bond replacement that retains the dipolar characteristics of the C═O bond of a peptide, but lacks the hydrogen bond donating ability of the N−H group. The similarity between the CFA2 conformer and $C7_{eq}$ of ADA suggests that this dipolar characteristic is enough to orient an adjacent native peptide bond or be oriented by an adjacent peptide moiety as the case may be, in a fashion not very different from that seen in ADA. A similar situation may be present in cases of other peptide replacements that possess a component that mimics the C═O bond dipole but lack an NH hydrogen bond donor (*N*-alkyl peptides, for example).[46,47]

There are also other conformations among the gas phase minima found for CFA that bear resemblance to alanine dipeptide analogue conformations that have previously been reported. For example, the CFA3 conformation is found to be only 1.16 kcal/mol above the ground state at the highest level of theory employed here. This conformation closely matches the α_R conformation of ADA which was found to lie 3.2 kcal/mol above the ground state by Wang and Duan (called α_L in the Kaminsky/Jensen study). The backbone dihedral angles of ADA α_L (−83°, −10°)[36] are mimicked very well by CFA3 (−90.5°, −5.26°). CFA5, 2.28 kcal/mol above the ground state, is similar to the ϵ_D ADA conformation reported by Kaminsky and Jensen and identified as α_D by Wang and Duan. The ADA version of this conformation has Φ, Ψ values of 53.0°, −133.4° compared to 60.3°, −120.4° for CFA5. These results indicate that the intrinsic conformational profile of the alanine dipeptide analogue, which serves as a model for larger peptides, is better represented by CFA than DFA. This is perhaps not surprising given that DFA contains two peptide bond replacements and CFA retains a peptide linkage and incorporates only one fluoroalkene replacement.

Table 9 contains the relative energies and dihedral angle information for CFA in the aqueous phase. The CFA1 conformation is found to be the global minimum in the gas phase as it was in the aqueous phase. The backbone dihedral angles of the minimum found in the aqueous phase (−88.4°, 117.6°) are very similar it those of the gas phase CFA1 (−80.9°, 113.1), and there are only subtle differences in the important interatomic distances. For example, the distance between the carbonyl

oxygen and the vinylic hydrogen opens up from 3.2740 to 3.4904 Å in going from gas to aqueous phase. Presumably, in the absence of a dielectric continuum, there are stronger electrostatic interactions between these partially charged atoms. Interestingly, the CFA2 conformation is not found to be a minimum on the aqueous phase potential energy surface. All attempts to locate this structure in the aqueous phase optimizations led to the CFA1 structure. The major difference between the two conformations involves rotation about Φ thus rotating the peptide moiety. Presumably, it is the hydration of the peptide moiety that results in the loss of CFA2 as a minimum in the presence of an aqueous medium.

Conformations CFA3, CFA4, CFA5, CFA6, and CFA8 are all found to be minima in the aqueous phase and possess structures that are closely related to their gas phase counterparts with backbone dihedral angles that are well within 10°. CFA7 is not found to be a minimum on the aqueous phase potential energy surface. Upon optimization, this structure moves to the CFA3 conformation in the aqueous phase.

The picture that emerges for CFA in the aqueous phase is that there are three conformations (CFA1, CFA3, CFA4) that are within 0.49 kcal/mol of the ground state at the MP2-III level of theory. In the gas phase, conformations CFA1 through CFA4 span a gap of 1.16 kcal/mol. In both the gas and aqueous phase, conformations CFA5 through CFA8 are significantly higher in energy and are not expected to be highly populated under either condition. Clearly, the most significant difference between the gas and aqueous phase conformational landscape for this system is the loss of CFA2 from the aqueous phase.

As discussed above for the DFA system, in addition to comparing the conformational profile of the mimic to that of ADA, we are also interested in evaluating the performance of more computationally efficient methods (MMFF and B3LYP) by comparing the results to those obtained with the highest-level ab initio methods used in this study. For the CFA1 system, B3LYP/6-31+G(d) does a reasonable job of representing the MP2-III results with some notable differences. B3LYP captures the essence of the CFA conformational profile in that it places CFA5 through CFA8 far above the low-energy conformations among CFA1 through CFA4. However, CFA2 is not found on the B3LYP conformational energy surface in either the gas or aqueous phases. Also, the energetic ordering of CFA3 and CFA4 is reversed in the aqueous phase relative to the MP2-III result. The story is more complex with MMFF (as implemented in Macromodel). In the gas phase, it does not find CFA1 as a minimum. CFA2 is found to be the global minimum instead. Also, CFA3 is not found as a minimum on the CFA gas phase potential. In addition, a conformation, designated CFA4m, which is not well represented by any of the existing CFA conformations but is somewhat similar to β_{anti} sheet, is found by MMFF. In the aqueous phase, MMFF finds a number of conformations that are different from those identified from the other studies. These are identified in Table 7 as CFA9m through CFA11m. If a particular structure was deemed to be somewhat related to one of the existing ones, this was indicated in the nomenclature (for example, CFA8m is related to the CFA8 conformation). The MMFF aqueous phase ground state, CFA9m, has backbone dihedrals of −153.6°, 117.5° in comparison to the −88.4°, 117.6° values for CFA1. The CFA2 conformation is not found to exist as a minimum on the aqueous phase MMFF potential energy surface.

Alanine Dipeptide Analogue: N-Terminal Peptide Bond Replacement (NFA). Figure 8 shows the gas phase minima that were found for the peptidomimetic where the N-terminal peptide bond of alanine dipeptide analogue has been replaced by a fluoroalkene moiety, NFA. The energies and backbone dihedral angles for this set of conformations can be found in Table 10 for the gas phase and Table 11 for the aqueous phase (with thermochemical corrections for each in the Supporting Information). The MP2/6-311+G(d,p) optimizations of a large number of initial structures resulted in only six conformations. Two low-energy conformations, NFA1 and NFA2, are found at 0.00 and 0.49 kcal/mol, respectively, at the MP2-III level. The remaining conformations all lie significantly higher in energy. The NFA1 structure closely resembles the $C7_{eq}$ conformation that is the gas phase global minimum for ADA. The NFA1 Φ,Ψ values of −92.4°, 85.3° compare very favorably with the literature ADA values (−82°, 76°[36] and −82.0°, 80.6°[16]) for the calculations in the absence of solvent. This structure provides a better mimic of the $C7_{eq}$ ADA structure than CFA2 (see Figure 7). The C−F---H−N interaction appears to be a better representation of the C═O---H−N interaction than the C═O---H−C interaction in CFA2. As indicated in Figure 8, the F---H distance of this interaction is 2.407 Å, which indicates a much stronger interaction compared to the 3.774 Å value for the O---H distance in CFA2. Thus, it would appear, at least based on the intrinsic conformational preferences in the absence of a surrounding medium, that replacing the C-terminal peptide linkage of alanine dipeptide analogue with a fluoroalkene represents a greater conformational perturbation than replacing the N-terminal peptide. The NFA2 structure is also found to be very low in energy. In this structure, the mean plane of the fluoroalkene is nearly perpendicular to that of the peptide moiety, and the NH bond vector of the peptide points toward the fluoroalkene with the carbonyl O oriented away from it.

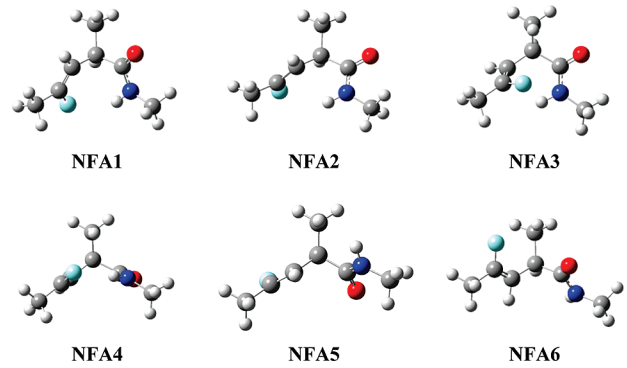

Figure 8. MP2/6-311+G(d,p) geometries for the energy minima that were found for NFA in the gas phase.

The remaining conformations are significantly higher in energy, but some also resemble ADA conformations. For example, NFA3 (53.5°, 36.8°) is similar to the α_L (63.2°, 35.4°) conformation of the Wang/Duan ADA study (which is denoted α_D in the Kaminsky/Jensen study of ADA). It also bears close resemblance to the standard left-handed helix structure (Table 4). Also, NFA4 (79.6, −69.3) is very similar to the $C7_{ax}$ conformation of ADA (Kaminsky/Jensen, 74°, −54°; Wang/Duan, 75.8°, −62.8°). This conformation is an interesting structure because it possesses an intramolecular hydrogen bond between the H−N of the C-terminal peptide and the C═O of the N-terminal peptide. The structure is shown in Figure 5, and an alternate view is presented in Figure 9 with a direct comparison to NFA4. The interatomic F---H distance of 2.102 Å in the fluoroalkene mimic is longer than the corresponding value in the native alanine dipeptide analogue (1.886 Å), but, clearly, the NFA4 conformation captures the salient features of the $C7_{ax}$ conformation.

TABLE 10: Relative Energies (Δ*E*, in kcal/mol) and Torsion Angles for Gas Phase Conformations of NFA

				ΔE				
	Φ[a]	Ψ[a]	μ[b]	MP2-I[c]	MP2-II[d]	MP2-III[e]	B3LYP[f]	MMFF[g]
NFA1	−92.4	85.3	3.56	0.00	0.00	0.00	0.00	0.00
NFA2	−111.5	25.0	4.84	0.89	0.60	0.42	0.45	5.89
NFA3	53.5	36.8	5.51	2.55	2.19	2.17	3.18	4.53
NFA4	79.6	−69.3	4.20	2.80	2.62	2.67	2.96	2.21
NFA5	−118.0	−85.34	5.10	3.25	3.42	3.26	3.09	5.31
NFA6	101.4	100.4	4.88	4.91	4.88	4.80	4.82	4.17
NFA7m[h]	154.1	125.1						3.67
NFA8m[h]	164.2	148.4						4.45
NFA9m[h]	−21.0	93.7						5.08
NFA10m[h]	110.8	−151.5						5.09
NFA11m[h]	81.3	66.2						5.17
NFA12m[h]	−45.5	−52.7						6.06

[a] Dihedral angle, in degrees. [b] Dipole moment, in debeye. [c] MP2-I = MP2/6-311+G(d,p)//MP2/6-311+G(d,p). [d] MP2-II = MP2/aug-cc-pVDZ//MP2/6-311+G(d,p). [e] MP2-III = MP2/aug-cc-pVTZ//MP2/6-311+G(d,p). [f] B3LYP/6-31+G(d)//B3LYP/6-31+G(d). [g] As implemented in Maestro (v6.5)/Macromodel-Batchmin (v8.6). [h] Found as a minimum only in MMFF optimizations. Torsion angles from the MMFF structure.

TABLE 11: Relative Energies (Δ*E*, in kcal/mol) and Torsion Angles for Aqueous Phase Conformations of NFA

			ΔE				
	Φ[a]	Ψ[a]	MP2-I[b]	MP2-II[c]	MP2-III[d]	B3LYP[e]	MMFF[f]
NFA1	−123.9	120.0	0.00	0.00	0.00	0.00	0.00
NFA2							
NFA3	45.9	54.2	2.72	2.17	2.26	3.42	1.84
NFA4	106.8	−83.3	4.90	4.43	4.55	4.18	
NFA5	−102.6	−51.7	1.95	1.92	1.88	1.78	1.42
NFA6	96.6	113.2	3.06	2.82	2.87	3.18	1.55
NFA7	−93.3	−28.6	1.77	1.46	1.43	1.68	
NFA8m[g]	−115.5	152.5					0.41
NFA9m[g]	116.1	87.8					1.38
NFA10m[g]	116.5	146.1					1.39
NFA11m[g]	−18.9	−91.7					3.46
NFA12m[g]	175.5	−72.3					3.78

[a] Dihedral angle, in degrees. [b] MP2-I = MP2/6-311+G(d,p)//MP2/6-311+G(d,p). [c] MP2-II = MP2/aug-cc-pVDZ//MP2/6-311+G(d,p). [d] MP2-III = MP2/aug-cc-pVTZ//MP2/6-311+G(d,p). [e] B3LYP/6-31+G(d)//B3LYP/6-31+G(d). [f] As implemented in Maestro (v6.5)/Macromodel-Batchmin (v8.6). [g] Found as a minimum only in MMFF optimizations. Angles reported in the table are MMFF values.

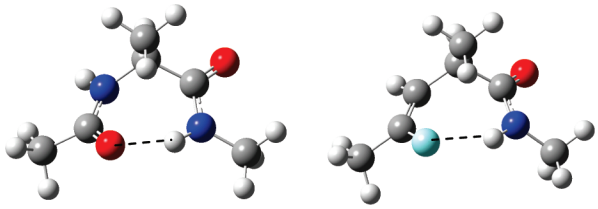

Figure 9. $C7_{ax}$ conformation of ADA (left) from the Kaminsky/Jensen study[36] at MP2/aug-cc-pVDZ compared to NFA4 (right) from this work (MP2/6-311+G(d,p). The interatomic distances indicated by the dashed lines are 1.886 (left) and 2.102 (right) Å.

Thus, compared to DFA and CFA, the NFA system provides the clearest examples of conformations where interactions that mimic the familiar intramolecular hydrogen bonding interactions between adjacent peptide groups in the alanine dipeptide analogue can be identified. These kinds of interactions are present in both NFA1 and NFA4 mimicking those of $C7_{eq}$ and $C7_{ax}$, respectively, in ADA. Previous work[15,48−50] has indicated that the C−F bond is not expected to be nearly as effective a hydrogen bond acceptor as the C═O group in the native peptide. It is interesting to note, however, that the energy gap between these two conformations is calculated to be nearly the same in their respective systems. For ADA, $C7_{ax}$ is been found to be approximately 2.5 kcal/mol above the ground state $C7_{eq}$.[16,36] In this work, with MP2-III, the corresponding NFA4 is found to be 2.67 kcal/mol above the ground state NFA1 in the gas phase. Also, examination of both of the possible single-replacement compounds, CFA and NFA, indicates that the combination of a native N−H hydrogen bond donor and a C−F replacement acceptor (as in NFA1, NFA4) seems to be a better representation of a hydrogen bond than the alternative where the C═O acceptor is retained and the N−H donor been replaced by a vinylic C−H group (as in CFA2).

The aqueous phase results for the NFA system are shown in Table 11. The NFA1 conformation is found to be the global minimum as it was in the gas phase. The backbone dihedral angles in the aqueous phase are substantially different from the gas phase version of the structure. They change from −92.4°, 85.3° to −123.9°, 120.0° which corresponds to the structure opening up to a more extended backbone (i.e., becoming more like the C5 (β_L) structure (Table 3) or like a standard parallel β sheet (Table 4)). The Wang/Duan study reports dihedral angles for both gas phase and aqueous phase conformations of ADA (Table 3). The $C7_{eq}$ conformation is −82.0°, 80.6° in the gas phase and −86.3°, 90.1° in the aqueous phase structure. Thus, the effect of aqueous hydration is the same as what is seen here with NFA1, but the magnitude of the effect is far less significant. The NFA2 conformation is not found as a minimum on the aqueous MP2/6-311+G(d,p) potential energy surface. The next highest energy conformer in the aqueous phase is NFA7 which resembles the α_R structure of the Wang/Duan[16] ADA study (which is called α_L in the Kaminsky/Jensen[36] study). This is a

new conformer that was not found to be a minimum in the gas phase studies. NFA7 is predicted to lie 1.43 kcal/mol above the ground state with MP2-III.

The impact of hydration causes other shifts in relative conformational energy ordering. The NFA4 structure, which resembles $C7_{ax}$ of ADA, increases significantly in relative energy, from 2.67 to 4.55 kcal/mol at the highest level of theory employed here. Other conformations become more competitive upon the consideration of hydration effects. For example, at MP2-III, NFA6 goes from a relative energy in the gas phase of 4.80 to 2.87 kcal/mol. NFA5 goes from 3.26 to 1.88 kcal/mol. NFA3, which is similar to the standard left-handed helix, has roughly the same relative energy in the gas phase is in the aqueous.

Tables 10 and 11 allow for an assessment of the performance of B3LYP/6-31+G(d) and MMFF, relative to that of MP2/aug-cc-pVTZ//MP2/6-311+G(d,p) (MP2-III) for the NFA system. The B3LYP/6-31+G(d,) results closely mirror the higher-level ab initio results in both the gas phase and in aqueous solution. Most of the B3LYP relative energies are within tenths of a kcal/mol of the MP2-III results. The exception is the NFA3 conformation whose relative energy is slightly overestimated by B3LYP compared to the MP2-III results. The trends in going from the gas phase to the aqueous phase are also well represented by the PCM-B3LYP results. MMFF does predict NFA1 to be the ground state conformation in the both the gas and aqueous phases. However, NFA2, predicted to be very close to the minimum in the gas phase with the quantum mechanical methods, is predicted with MMFF to be 5.89 kcal/mol above the minimum. Also, as seen in the CFA system, a large number of additional conformations (denoted NFA7m through NFA12m) are found to be minima on the MMFF potential surface that are not found to be minima with the quantum mechanical methods.

Conclusions

A computational investigation using high levels of ab initio theory as well as more computationally efficient methods has been conducted to investigate the conformational ramifications of substitution of a peptide bond by a fluoroalkene moiety thus generating a peptidomimetic. This is a follow-up study to the investigation of the hydrogen bonding tendencies of fluoroalkene peptidomimetics reported previously in this journal.[15]

The alanine dipeptide (ADA) analogue was employed as a model peptide compound. It was found that replacement of both of the peptide bonds of ADA, thus generating DFA, resulted in a significant impact on the predicted conformational profile of the molecule. DFA does not assume conformations that are representative of the intramolecularly hydrogen-bonded conformations that have been identified previously as an important aspect of the intrinsic (in the absence of interacting solvent) ADA conformational profile. Also, the conformational profile of DFA shows little solvent dependence, while that of ADA shows a great deal of dependence on the surrounding medium. The solvent dependence in ADA is due in large part to the fact that folded intramolecularly hydrogen-bonded structures compete well in the absence of an aqueous medium, but more extended conformations, which allow polar groups to be adequately hydrated, are important in the presence of an aqueous phase. The absence of strong intramolecular attractions in DFA makes it prefer extended conformations in both scenarios.

Peptide mimics that retain one of the two peptide bonds of ADA were also investigated. In the CFA model peptide mimic, the C-terminal peptide bond was replaced with a fluoroalkene and the N-terminal peptide bond retained. For CFA, four conformations were found in the absence of solvent to be within 1.16 kcal/mol of the ground state. The lowest-energy structure bears some resemblance to the $C7_{eq}$ conformer of ADA which has been identified as the ground state conformation of ADA in the gas phase, and the next highest energy structure bears resemblance to the next highest, $C5(\beta_L)$, in the series of ADA conformations in the gas phase. However, in the aqueous phase, this conformation disappears from the conformational energy surface for CFA. The alternative singly substituted mimic, NFA, which contains a fluoroalkene replacement of the N-terminal peptide bond of ADA, is predicted to possess a conformational profile that reflects key attributes of that of ADA. For example, conformational minima were obtained for NFA with an arrangement of the C−F---H−N bond vectors that closely mimics the intramolecular hydrogen bond in the $C7_{eq}$ and $C7_{ax}$ conformations of the ADA dipeptide. The geometry indicates that the intramolecular interaction is not as tight in the case of the fluoroalkene mimic, but the relative energy of the two conformations in the mimic is very similar to that of ADA. In aqueous solvent, an extended, β-sheet-like structure predominates.

If one were to investigate with a computational approach the conformational preferences of much larger peptidic systems that incorporate fluoroalkenes as selected peptide bond replacements, one would need a much more computationally efficient method than the ab initio calculations reported here. For this reason, results were also obtained with the MMFF force field and the B3LYP/6-31+G(d) approach. In general, the conformational preferences at the MP2/aug-cc-pVTZ//MP2/6-311+G(d,p) level were quite well represented by the B3LYP/6-31+G(d) results. The force field calculations with MMFF were able to capture many of the salient features of the conformational profile, but with occasional significant discrepancies.

Acknowledgment. Financial support for this work was provided from the Naval Academy Research Council. B.E.M. received support from Naval Academy Research Office/ONR. A grant of computing time was also received from the DoD High Performance Computing Modernization Program. This support is gratefully acknowledged.

Supporting Information Available: MP2/aug-cc-pVTZ//MP2/6-311+G(d,p) relative energies, including thermochemical corrections for CFA and NFA. This material is available free of charge via the Internet at http://pubs.acs.org.

References and Notes

(1) Lin, J.; Toscano, P. J.; Welch, J. T. *Proc. Natl. Acad. Sci. U.S.A.* **1998**, *95*, 14020.
(2) Ng, P.-S.; Bergstrom Donald, E. *Nano Lett.* **2005**, *5*, 107.
(3) Wipf, P.; Henninger, T. C.; Geib, S. J. *J. Org. Chem.* **1998**, *63*, 6088.
(4) Arnt, L.; Rennie, J. R.; Linser, S.; Willumeit, R.; Tew, G. N. *J. Phys. Chem. B* **2006**, *110*, 3527.
(5) Van der Veken, P.; Senten, K.; Kertesz, I.; De Meester, I.; Lambeir, A.-M.; Maes, M.-B.; Scharpe, S.; Haemers, A.; Augustyns, K. *J. Med. Chem.* **2005**, *48*, 1768.
(6) Niida, A.; Tomita, K.; Mizumoto, M.; Tanigaki, H.; Terada, T.; Oishi, S.; Otaka, A.; Inui, K.-I.; Fujii, N. *Org. Lett.* **2006**, *8*, 613.
(7) Vasbinder, M. M.; Jarvo, E. R.; Miller, S. J. *Angew. Chem., Int. Ed.* **2001**, *40*, 2824.
(8) Vasbinder, M. M.; Miller, S. J. *J. Org. Chem.* **2002**, *67*, 6240.
(9) Bartlett, P. A.; Otake, A. *J. Org. Chem.* **1995**, *60*, 3107.
(10) Boros, L. G.; Corte, B. D.; Gimi, R. H.; Welch, J. T.; Wu, Y.; Handschumacher, R. E. *Tetrahedron Lett.* **1994**, *35*, 6033.
(11) Cieplak, P.; Kollman, P. A.; Radomski, J. P. *ACS Symp. Ser.* **1996**, *639*, 143.
(12) Cox, D. G.; Gurusamy, N.; Burton, D. J. *J. Am. Chem. Soc.* **1985**, *107*, 2811.

(13) Okada, M.; Nakamura, Y.; Saito, A.; Sato, A.; Horikawa, H.; Taguchi, T. *Tetrahedron Lett.* **2002**, *43*, 5845.
(14) Otaka, A.; Watanabe, H.; Yukimasa, A.; Oishi, S.; Tamamura, H.; Fujii, N. *Tetrahedron Lett.* **2001**, *42*, 5443.
(15) Urban, J. J.; Tillman, B. G.; Cronin, W. A. *J. Phys. Chem. A* **2006**, *110*, 11120.
(16) Wang, Z. X.; Duan, Y. *J. Comput. Chem.* **2004**, *25*, 1699.
(17) Mehta, M. A.; Fry, E. A.; Eddy, M. T.; Dedeo, M. T.; Anagnost, A. E.; Long, J. R. *J. Phys. Chem. B* **2004**, *108*, 2777.
(18) Takekiyo, T.; Imai, T.; Kato, M.; Taniguchi, Y. *Biopolymers* **2004**, *73*, 283.
(19) Chang, G.; Guida, W. C.; Still, W. C. *J. Am. Chem. Soc.* **1989**, *111*, 4379.
(20) Saunders, M.; Houk, K. N.; Wu, Y.-D.; Still, W. C.; Lipton, M.; Chang, G.; Guida, W. C. *J. Am. Chem. Soc.* **1990**, *112*, 1419.
(21) Mohamadi, F.; Richards, N. G. J.; Guida, W. C.; Liskamp, R.; Lipton, M.; Caufield, C.; Chang, G.; Hendrickson, T.; Still, W. C. *J. Comput. Chem.* **1990**, *11*, 440.
(22) Halgren, T. A. *J. Comput. Chem.* **1996**, *17*, 490.
(23) Halgren, T. A. *J. Comput. Chem.* **1996**, *17*, 520.
(24) Halgren, T. A. *J. Comput. Chem.* **1996**, *17*, 553.
(25) Halgren, T. A. *J. Comput. Chem.* **1996**, *17*, 615.
(26) Halgren, T. A.; Nachbar, R. *J. Comput. Chem.* **1996**, *17*, 587.
(27) Hasel, W.; F., H. T.; Still, W. C. *Tetrahedron Comput. Method* **1988**, *1*, 103.
(28) Frisch, M. J.; Trucks, G. W.; Schlegel, H. B.; Scuseria, G. E.; Robb, M. A.; Cheeseman, J. R.; Montgomery, J. A., Jr.; Vreven, T.; Kudin, K. N.; Burant, J. C.; Millam, J. M.; Iyengar, S. S.; Tomasi, J.; Barone, V.; Mennucci, B.; Cossi, M.; Scalmani, G.; Rega, N.; Petersson, G. A.; Nakatsuji, H.; Hada, M.; Ehara, M.; Toyota, K.; Fukuda, R.; Hasegawa, J.; Ishida, M.; Nakajima, T.; Honda, Y.; Kitao, O.; Nakai, H.; Klene, M.; Li, X.; Knox, J. E.; Hratchian, H. P.; Cross, J. B.; Adamo, C.; Jaramillo, J.; Gomperts, R.; Stratmann, R. E.; Yazyev, O.; Austin, A. J.; Cammi, R.; Pomelli, C.; Ochterski, J. W.; Ayala, P. Y.; Morokuma, K.; Voth, G. A.; Salvador, P.; Dannenberg, J. J.; Zakrzewski, V. G.; Dapprich, S.; Daniels, A. D.; Strain, M. C.; Farkas, O.; Malick, D. K.; Rabuck, A. D.; Raghavachari, K.; Foresman, J. B.; Ortiz, J. V.; Cui, Q.; Baboul, A. G.; Clifford, S.; Cioslowski, J.; Stefanov, B. B.; Liu, G.; Liashenko, A.; Piskorz, P.; Komaromi, I.; Martin, R. L.; Fox, D. J.; Keith, T.; Al-Laham, M. A.; Peng, C. Y.; Nanayakkara, A.; Challacombe, M.; Gill, P. M. W.; Johnson, B.; Chen, W.; Wong, M. W.; Gonzalez, C.; Pople, J. A. *Gaussian03*, revision E.01; Gaussian, Inc: Wallingford, CT, 2004.
(29) Møller, C.; Plesset, M. S. *Phys. Rev.* **1934**, *46*, 618.
(30) Becke, A. D. *Phys. Rev. A: At., Mol., Opt. Phys.* **1988**, *38*, 3098.
(31) Lee, C.; Yang, W.; Parr, R. G. *Phys. Rev.* **1988**, *B37*, 785.
(32) Cances, E.; Mennucci, B.; Tomasi, J. *J. Chem. Phys.* **1997**, *107*, 3032.
(33) Cossi, M.; Barone, V.; Mennucci, B.; Tomasi, J. *Chem. Phys. Lett.* **1998**, *286*, 253.
(34) Mennucci, B.; Tomasi, J. *J. Chem. Phys.* **1997**, *106*, 5151.
(35) Cossi, M.; Scalmani, G.; Rega, N.; Barone, V. *J. Chem. Phys.* **2002**, *117*, 43.
(36) Kaminsky, J.; Jensen, F. *J. Chem. Theory Comput.* **2007**, *3*, 1774.
(37) IUPAC-IUB Commission on Biochemical Nomenclature. Abbreviations and symbols for the description of the conformation of polypeptide chains. Tentative rules (1969). *Biochemistry*, **1970**, *9*, 3471.
(38) Voet, D.; Voet, J. G. *Biochemistry*; John Wiley and Sons: Hoboken, NJ, 2004.
(39) Zhao, Y.; Truhlar, D. G. *Acc. Chem. Res.* **2008**, *41*, 157.
(40) Antony, J.; Grimme, S. *Phys. Chem. Chem. Phys.* **2006**, *8*, 5287.
(41) Schreiner, P. R. *Angew. Chem., Int. Ed.* **2007**, *46*, 4217.
(42) Gnanakaran, S.; Hochstrasser, R. M. *J. Am. Chem. Soc.* **2001**, *123*, 12886.
(43) Lee, M.-E.; Lee, S. Y.; Joo, S.-W.; Cho, K.-H. *J. Phys. Chem. B* **2009**, *113*, 6894.
(44) Madison, V.; Kopple, K. D. *J. Am. Chem. Soc.* **1980**, *102*, 4855.
(45) Han, W.-G.; Jalkanen, K. J.; Elstner, M.; Suhai, S. *J. Phys. Chem. B* **1998**, *102*, 2587.
(46) Subtelny, A. O.; Hartman, M. C. T.; Szostak, J. W. *J. Am. Chem. Soc.* **2008**, *130*, 6131.
(47) Shah, N. H.; Butterfoss, G. L.; Nguyen, K.; Yoo, B.; Bonneau, R.; Rabenstein, D. L.; Kirshenbaum, K. *J. Am. Chem. Soc.* **2008**, *130*, 16622.
(48) Alkorta, I.; Rozas, I.; Elguero, J. *J. Fluorine Chem.* **2000**, *101*, 233.
(49) Dunitz, J. D.; Taylor, R. *Chem.—Eur. J.* **1997**, *3*, 89.
(50) Howard, J. A. K.; Hoy, V. J.; O'Hagan, D.; Smith, G. T. *Tetrahedron* **1996**, *52*, 12613.

JP9094535